Generation of solitons and breathers in the extended Korteweg–de Vries equation with positive cubic nonlinearity

R. Grimshaw,[1] A. Slunyaev,[2,a)] and E. Pelinovsky[2]
[1]*Department of Mathematical Sciences, Loughborough University, Loughborough LE11 3TU, United Kingdom*
[2]*Department of Nonlinear Geophysical Processes, Institute of Applied Physics, Russian Academy of Sciences, Nizhny Novgorod 603950, Russia*

(Received 23 October 2009; accepted 2 December 2009; published online 5 January 2010)

The initial-value problem for box-like initial disturbances is studied within the framework of an extended Korteweg–de Vries equation with both quadratic and cubic nonlinear terms, also known as the Gardner equation, for the case when the cubic nonlinear coefficient has the same sign as the linear dispersion coefficient. The discrete spectrum of the associated scattering problem is found, which is used to describe the asymptotic solution of the initial-value problem. It is found that while initial disturbances of the same sign as the quadratic nonlinear coefficient result in generation of only solitons, the case of the opposite polarity of the initial disturbance has a variety of possible outcomes. In this case solitons of different polarities as well as breathers may occur. The bifurcation point when two eigenvalues corresponding to solitons merge to the eigenvalues associated with breathers is considered in more detail. Direct numerical simulations show that breathers and soliton pairs of different polarities can appear from a simple box-like initial disturbance. © *2010 American Institute of Physics*. [doi:10.1063/1.3279480]

Internal solitary waves in the stratified coastal ocean are ubiquitous and are commonly observed. They may reach an amplitude of 100 m and be comparable to the water depth. The solitary waves preserve their shape and propagate for long distances unchanged, thus they play a very important role in the distribution of energy in the ocean interior. Another kind of nonlinear internal wave, bounded nonlinear wave packets or *breathers*, are already known as exact solutions of certain model nonlinear wave evolution equations, such as the modified Korteweg–de Vries (KdV) equation. In the stratified ocean, the existence of breathers needs a specific kind of stratification (quite distinct from the popular two-layer model). The possibility of internal breathers in a stratified fluid was only recently confirmed by fully nonlinear numerical simulations. In general breathers are more complicated nonlinear waves compared with solitary waves and have been much less investigated. The Gardner equation (GE) (the KdV equations with an extra term with cubic nonlinearity) is a simple nonlinear wave model which governs the dynamics of internal wave breathers. Getting the benefit from the integrability of the GE by means of the inverse scattering technique (IST), we study the initial-value problem for a box-shaped initial perturbation in detail, analytically and numerically. We show that when the perturbation is of the opposite sign than the usual KdV solitary waves, a complicated scenario occurs. Single solitary waves, pairs of solitary waves, and internal breathers may be born from this simple initial disturbance, depending on its amplitude and width.

a)Author to whom correspondence should be addressed. Electronic mail: slunyaev@hydro.appl.sci-nnov.ru.

I. INTRODUCTION

Internal solitary waves have often been modeled as solitons of the KdV type (see reviews in Refs. 1–3). These models can provide for an accurate description of internal solitary wave propagation and their interactions. In particular, the solitary waves in the KdV equation can be found as the asymptotic outcome from a localized initial disturbance (see Ref. 4, for instance). Moreover, KdV solitons are often convenient for a qualitative description of nonlinear wave dynamics. Hence the KdV model is popular in many physical applications.

For the case of internal waves, the coefficients in the KdV equation are defined by the density stratification, which may be quite variable in the ocean, and can lead to different signs of the coefficient of the quadratic nonlinear term in the KdV equation. Indeed, this coefficient can be quite small and may even vanish. In this scenario the quadratic and cubic nonlinear terms appear at the same order in an asymptotic perturbation theory, and the outcome is an extended KdV equation (or the GE), with both quadratic and cubic nonlinear terms. Although it is slightly more complicated than the KdV equation, in many cases it can describe large-amplitude internal solitary waves rather better, showing dynamics which can look quite different from the KdV case.[5,6] The GE is also integrable, and thus allows the analysis using the IST.[4]

The associated scattering problem for the KdV equation is defined by the stationary Schrödinger equation, which plays a fundamental role in quantum physics. Thus, the initial-value problem for the KdV equation is very well established and understood. In contrast, the initial-value problem for the GE is less well developed. An example of its

rather more complicated dynamics was shown by Grimshaw *et al.*;[7] the solution becomes more intricate due to the competition between the two nonlinear terms. In the case of a positive coefficient of the cubic nonlinear term relative to the sign of the coefficient of the linear dispersive term, as well as solitons, there are allowed exact breather solutions. The coefficients of the equation are determined by the density stratification;[3,8] the cubic nonlinear coefficient is positive, for example, in the case of a three-layer fluid, when the density jumps are situated close to the bottom and to the surface, see Grimshaw *et al.*[8] A breather is essentially a nonlinear wave packet, and its dynamics can be quite complicated.[6,9–11] The possibility of the presence of breather waves in realistic conditions in a continuously stratified ocean was shown recently through fully nonlinear numerical simulations by Lamb *et al.*[12]

Our concern in this paper is to examine which kind of initial conditions can generate breathers. Internal solitary waves can become coupled due to weak dispersion or dissipation effects,[13,14] which is one possible mechanism for the formation of internal breathers. Breather-type waves may also appear due to the modulational instability of intense short-scale waves,[11,15] through perturbations of solitary waves,[9] or through variations in the waveguide characteristics.[16] However, steepening of internal tides is the most common mechanism for the generation of internal solitary waves in the ocean, and so here we shall study the generation of intense internal breathers from initial disturbances of rather simple shapes.

We have already noted that the initial-value problem for the GE is more complicated than for the KdV equation[7] (see also the discussion in Sec. II). The initial-value problem in the large-amplitude limit (using then the framework of the modified KdV equation) coincides with that for the focusing nonlinear Schrödinger (NLS) equation, which is widely used in nonlinear optics, and we note the long but still incomplete list of the papers studying the initial value problem for the focusing NLS equation.[17–27] It is significant that the KdV-like evolution equations describe real-valued wave fields, while the NLS equation governs evolution of complex wave fields. Therefore not all the initial-value problems treated within the framework of the NLS equation have physical sense in our case.

Although NLS envelope solitons on a pedestal are often called breathers, in this paper we shall call breathers only solitary solutions of modified KdV equation (or the GE) corresponding to a pair of complex conjugate eigenvalues. One eigenvalue of the scattering problem for the NLS equation always corresponds to one envelope soliton. A pair of complex conjugate eigenvalues of the scattering problem for the NLS equation corresponds to two envelope solitons. The initial-value problem for disturbances composed of two adjoining box-like profiles was studied by Clarke *et al.*[25] and also by Kaup *et al.*[22] and Kaup and Malomed.[23] It was found that single eigenvalues appear when the boxes have similar polarities, while coupled complex conjugate pairs are favored by asymmetric initial pulses. Takahashi and Konno[21] and Desaix *et al.*[27] showed that complex conjugate pairs of eigenvalues can arise from two separated pulse disturbances.

In this paper we shall show that breathers of the GE, and also solitons of opposite polarities can be generated from a single box-shaped initial disturbance. Section II is introductory, where we formulate the associated scattering system for the GE, discuss its relation to the KdV and modified KdV equations, and present the soliton and breather solutions. In Sec. III the exact solution of the scattering problem for a box-like initial disturbance is obtained and discussed for both possible signs. In Sec. IV some results of the direct numerical simulations of the initial-value problem for the GE are presented. Our results are summarized in Sec. V.

II. EXACT SOLUTIONS OF THE GARDNER EQUATION

The GE with a positive coefficient of the cubic nonlinear term is written here in the usual dimensionless form

$$u_t + 6uu_x + 6u^2u_x + u_{xxx} = 0. \tag{1}$$

For the case when internal waves in a stratified ocean are concerned, the function $u(x,t)$ has the sense of the displacement of the isopycnals, x is the horizontal coordinate, and t is time (more details may be found, for example, in Ref. 3). The coefficients of the evolution equation are defined by the background density stratification and current. When the cubic nonlinear coefficient has the same sign as the linear dispersion coefficient, then the equation may always be reduced to the form (1) with the help of the scaling and Galilean transformations.

Equation (1) belongs to the important class of integrable equations. The long-time asymptotics of its solution may be found with the help of the IST. This method consists of the solution of the associated linear scattering problem. The latter may be given in the form (AKNS approach, see Refs. 28 and 4)

$$\Lambda\Psi = \lambda\Psi, \quad \text{where } \Psi = \begin{pmatrix} \psi_1 \\ \psi_2 \end{pmatrix}, \quad \Lambda = \begin{pmatrix} -\partial_x & u \\ u+1 & \partial_x \end{pmatrix}. \tag{2}$$

Here Ψ is the complex-valued vector eigenfunction, and λ is the complex-valued eigenvalue. In addition to Eq. (2), temporal evolution of the eigenfunctions is also prescribed by the IST (see Ref. 4), but is not used in this study. The eigenvalue problem in a similar form was first suggested in Ref. 29 for the GE with negative coefficient of the cubic nonlinear term.

It is well known that the linear transformation

$$q(x,t) = u\left(x - \tfrac{3}{2}t, t\right) + \tfrac{1}{2} \tag{3}$$

reduces solutions of GE (1) to the solutions of the modified KdV (mKdV) equation

$$q_t + 6q^2q_x + q_{xxx} = 0. \tag{4}$$

The mKdV equation (4) has its own scattering system:[30]

$$\Xi\Psi = \sigma\Psi, \quad \Xi = \begin{pmatrix} -\partial_x & q \\ q & \partial_x \end{pmatrix}. \tag{5}$$

With the use of transformation (3) this eigenvalue problem (5) may be directly applied for solving the GE, by seeking the solutions of the mKdV equation on a pedestal, similar to the approach of Romanova.[31] However, since the transforma-

tion (3) links the initial-value problem for the GE with a zero background to an initial-value problem for the modified KdV equation on a pedestal, it has not received much attention in the literature.

It may be shown that

$$\Lambda^2\Psi = \left(\Xi^2 - \tfrac{1}{4}\right)\Psi = \left(\sigma^2 - \tfrac{1}{4}\right)\Psi = \lambda^2\Psi, \tag{6}$$

where q is changed to $u+1/2$ in Eq. (5). Then the eigenvalues of the two scattering problems, Eqs. (2) and (5), are connected by

$$\lambda^2 = \sigma^2 - \tfrac{1}{4}. \tag{7}$$

The eigenvalue problem for the GE with negative cubic nonlinearity was reduced in Ref. 7 to the eigenvalue problem of the KdV equation, which is a classic one, and thus, is more convenient for qualitative analysis. Solutions of the GE with positive cubic nonlinearity (1) may be transformed through the relation

$$v(x,t) = u(1+u) + i\frac{\partial u}{\partial x}, \tag{8}$$

similar to the well-known Miura transformation, to solutions of the KdV equation

$$\frac{\partial v}{\partial t} + 6v\frac{\partial v}{\partial x} + \frac{\partial^3 v}{\partial x^3} = 0. \tag{9}$$

The associated scattering problem for the KdV equation (9) follows from Eq. (2),

$$\left(\frac{\partial^2}{\partial x^2} + v(x)\right)\psi = \lambda^2\psi, \quad \psi = \psi_1 + i\psi_2. \tag{10}$$

But although the eigenvalue problem (10) has the classical form, the change (8) makes the field v complex-valued. Hence the scattering problem (10) corresponds to an unusual case, when the potential is complex, and simple analogs cannot be drawn.

It is useful to introduce the change in variable

$$\psi = \psi_1 + i\psi_2, \quad \phi = \psi_1 - i\psi_2, \tag{11}$$

so that the system (2) becomes

$$\begin{aligned} -\frac{\partial\phi}{\partial x} + i\left(u+\frac{1}{2}\right)\phi &= \left(\lambda - \frac{i}{2}\right)\psi, \\ -\frac{\partial\psi}{\partial x} - i\left(u+\frac{1}{2}\right)\psi &= \left(\lambda + \frac{i}{2}\right)\phi. \end{aligned} \tag{12}$$

This more symmetrical form allows the elimination of either variable to yield the equivalent second order equations

$$\begin{aligned} \frac{\partial^2\phi}{\partial x^2} + [u(u+1) - \lambda^2]\phi - iu_x\phi = 0, \\ \frac{\partial^2\psi}{\partial x^2} + [u(u+1) - \lambda^2]\psi + iu_x\psi = 0. \end{aligned} \tag{13}$$

Note that the second equation here is just Eq. (10) recovered by a different approach. We note from Eq. (2) or Eq. (13) that if λ is an eigenvalue, then so are $-\lambda$ and λ^*, and so the eigenvalues typically occur as a quartet, and only one quadrant of the eigenvalue plane may be considered without loss of generality. It is convenient hereafter to restrict our interest to eigenvalues $\mathrm{Re}(\lambda) > 0$. The discrete spectrum of the scattering problem corresponds to solutions which decay at infinity; solitary waves (solitons) correspond to real-valued eigenvalues, and breathers to complex-valued eigenvalues. Next, from Eq. (13) it follows that for the discrete spectrum, we can obtain the integral identities

$$\begin{aligned} \int_{-\infty}^{\infty} |\phi_x|^2 + [\lambda^2 - u(u+1)]|\phi|^2 + iu_x|\phi|^2 dx = 0, \\ \int_{-\infty}^{\infty} |\psi_x|^2 + [\lambda^2 - u(u+1)]|\psi|^2 - iu_x|\psi|^2 dx = 0. \end{aligned} \tag{14}$$

Taking the imaginary part of these expressions yields

$$\begin{aligned} 2\lambda_R\lambda_I\int_{-\infty}^{\infty} |\phi|^2 dx &= -\int_{-\infty}^{\infty} u_x|\phi|^2 dx, \\ 2\lambda_R\lambda_I\int_{-\infty}^{\infty} |\psi|^2 dx &= \int_{-\infty}^{\infty} u_x|\psi|^2 dx, \end{aligned} \tag{15}$$

where $\lambda = \lambda_R + i\lambda_I$. Note that for a real eigenvalue when $\lambda_I = 0$, both integral terms on the right-hand side (RHS) must be zero.

Returning to the system in the form (2) we can construct the equation set for the squared eigenfunctions,

$$\begin{aligned} I_x &= 2uQ_2 - 2(u+1)Q_1 - 2\lambda_I J, \quad J_x = 2\lambda_I I, \\ Q_{1x} &= uI - 2\lambda_R Q_1, \quad Q_{2x} = -(u+1)I + 2\lambda_R Q_2, \end{aligned} \tag{16}$$

where

$$\begin{aligned} I &= \psi_1\psi_2^* + \psi_2\psi_1^*, \quad J = i(\psi_1\psi_2^* - \psi_2\psi_1^*), \\ Q_1 &= |\psi_1|^2, \quad Q_2 = |\psi_2|^2. \end{aligned} \tag{17}$$

Here Q_1, Q_2 are real and non-negative, and I, J are real valued. Note that $|\phi|^2 = Q_1 + Q_2 + J$, $|\psi|^2 = Q_1 + Q_2 - J$, and then the relations (16) can be used to give an alternative derivation of Eq. (15).

There are several consequences which can now be drawn. In particular if $u(u+1) < 0$ (that is $-1 < u < 0$) for $a < x < b$ where $u = 0$ for $x \geq a$, $x \leq b$ where either or both of a, b may be infinite, then the real and imaginary parts of Eq. (14) may be considered separately which leads to the condition $\lambda_R^2 < \lambda_I^2$ where $\lambda = \lambda_R + i\lambda_I$. It follows that there are no real eigenvalues, and hence only breathers can occur.

For the GE a soliton is given by

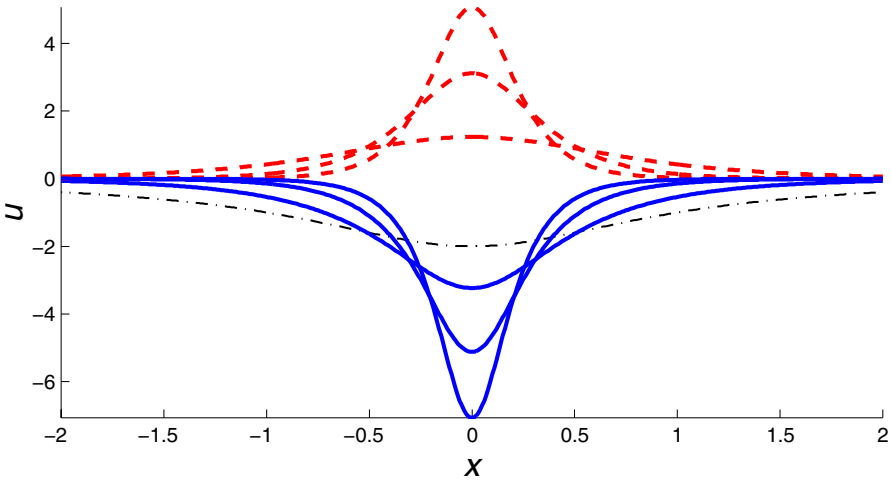

FIG. 1. (Color online) Solitons of the GE (1) (λ=0001, 1, 2, 3). The limiting algebraic soliton is given by the thin dashed-dotted black line.

$$u_S(x,t) = \frac{4\lambda^2}{1 \pm \sqrt{1+4\lambda^2}\cosh(2\lambda(x - x_0 - 4\lambda^2 t))}, \tag{18}$$

where the positive real number λ is the eigenvalue. The polarity of the solution cannot be determined by the eigenvalue alone, and instead needs information about the eigenfunctions. If the height of the wave is larger than $|A_{\rm lim}|, A_{\rm lim} = -2$ the soliton may have either polarity [depending on the choice of the sign ± in Eq. (18)], see Fig. 1. The negative soliton with limiting amplitude $A_{\rm lim}$ has a power-law decaying tail, plotted by the dashed-dotted line in Fig. 1, and is given by

$$u_{\rm alg}(x,t) = \lim_{\lambda\to 0} u_s(x,t) = -\frac{2}{1+x^2}. \tag{19}$$

The perturbed algebraic soliton (19) is known to be structurally unstable; it easily transforms to a breather.[9] Solitons of smaller amplitudes can only be positive.

The breather solution may be formally represented as an interaction of two solitons of different signs. One breather is determined by a couple of complex conjugated eigenvalues λ and λ^* and may be written in the form

$$u_{\rm BR}(x,t) = 2ab\frac{\dfrac{b\cosh\eta\cos\chi + a\cos\theta\cosh\varphi}{a\sin\theta\cosh\varphi + b\sinh\eta\cos\chi} + \dfrac{b\sinh\eta\sin\chi + a\sin\theta\sinh\varphi}{a\cos\theta\sinh\varphi - b\cosh\eta\sin\chi}}{\dfrac{b\cosh\eta\sin\chi - a\cos\theta\sinh\varphi}{a\sin\theta\cosh\varphi + b\sinh\eta\cos\chi} - \dfrac{b\sinh\eta\cos\chi + a\sin\theta\cosh\varphi}{a\cos\theta\sinh\varphi - b\cosh\eta\sin\chi}},$$

$$\eta = a(x - Vt - x_0), \quad \theta = b(x - vt - x_{\rm ph}),$$

$$V = a^2 - 3b^2, \quad v = 3a^2 - b^2, \tag{20}$$

$$\varphi + i\chi = \frac{1}{2}\ln\frac{i+2\lambda}{i-2\lambda}, \quad 2\lambda = a + ib.$$

The values x_0 and $x_{\rm ph}$ specify the initial position and phase of the breather. A breather is a two-parameter solution (real and imaginary parts of λ) and in general behaves like a wave packet propagating as a whole with velocity V, and with individual waves propagating with velocity v, so that V and v are essentially nonlinear analogs of the group and phase velocities, respectively. Note that depending on its parameters, a breather may propagate faster or slower than linear waves within the framework of the GE. The breather repeats its shape each time

$$T_{\rm BR} = \frac{\pi}{b(a^2+b^2)}. \tag{21}$$

If $a \gg b$ then the breather resembles two interacting solitons of different polarities [Fig. 2(a)]. The nonlinear wave is very asymmetric when a is not large. In the opposite case $b \gg a$ the envelope contains many individual waves and is rather symmetric [Fig. 2(b)].

Solitons and breathers elastically interact with each other and with other waves. The N-soliton exact solutions and

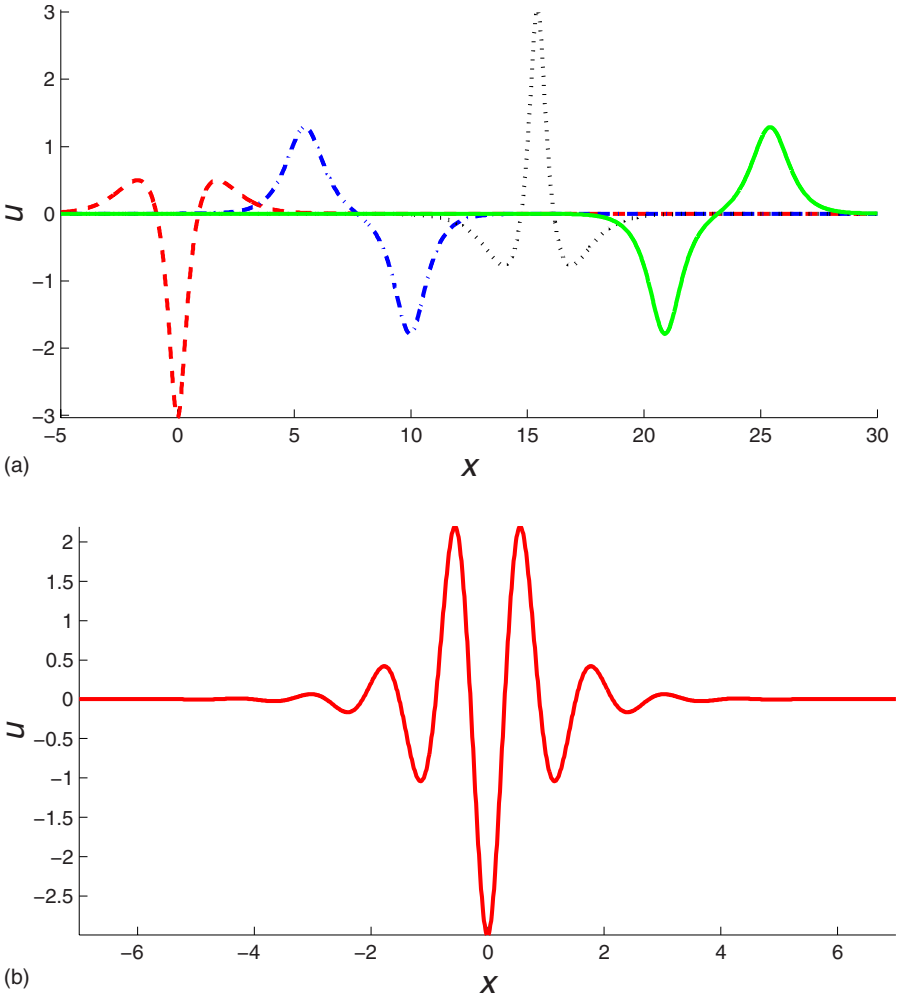

FIG. 2. (Color online) Breathers of the GE at different times: (a) quasi-interaction of two solitons ($\lambda = 3 \pm 0.2i$) plotted at times $t=0$, $T_{BR}/4$, $T_{BR}/2$, and $3T_{BR}/4$ from left to right; (b) a wave packet ($\lambda = 3 \pm 10i$).

mixed solitons-breathers may be found by different methods.[6,10,32]

III. INITIAL-VALUE PROBLEM: BOX IMPULSE

A simple configuration which allows analytic solution of the direct scattering problem (2) is represented by a square-wall-type disturbance with width L,

$$u(x,t=0) = \begin{cases} A, & |x| < L/2, \\ 0, & |x| \geq L/2. \end{cases} \tag{22}$$

This simplified wave profile is very convenient for an analytic study. However, similar shapes for internal tidal waves have been observed in realistic conditions, see Ref. 33.

For the box potential Eq. (15) can be reduced to

$$2\lambda_R\lambda_I \int_{-\infty}^{\infty} |\phi|^2 + |\psi|^2 dx = -8A\lambda_I |\psi_2|^2_{x=L/2}, \tag{23}$$

so that if $\lambda_I \neq 0$, there is a contradiction when $A > 0$. Hence for a positive box potential there can only be real eigenvalues. Also, the relations (16) can be used to show that

$$A\int_{-L/2}^{L/2} I dx = 2\lambda_R \int_{-L/2}^{\infty} Q_1 dx,$$

$$A\int_{-L/2}^{L/2} I dx + \int_{-L/2}^{\infty} I dx = 2\lambda_R \int_{-\infty}^{\infty} Q_2 dx, \tag{24}$$

$$2\lambda_I \int_{-L/2}^{\infty} I dx = 0,$$

where it is useful to note that in $x > L/2$, $\psi_1 = 2\lambda\psi_2$, $I = 4\lambda_R Q_2$, and in $x < -L/2$, $\psi_1 = 0$, $I = 0$. Then, since for $-1 < A < 0$, $\lambda_I \neq 0$, it follows that these can be rearranged to give

$$A\int_{-L/2}^{L/2} I dx = 2\lambda_R \int_{-L/2}^{\infty} Q_1 dx > 0,$$

$$\left(A + \frac{1}{2}\right)\int_{-L/2}^{L/2} I dx = 2\lambda_R \int_{-\infty}^{L/2} Q_2 dx > 0, \tag{25}$$

which are in contradiction when $-1/2 \leq A \leq 0$. Hence in this case there are no eigenvalues, real or complex valued. For

the case $-1 \le A < -1/2$ when only complex eigenvalues may occur, our numerical simulations of the GE and a perturbation analysis described below indicate that complex-valued eigenvalues do indeed exist, and so we infer that the nonexistence proof made above for $-1/2 \le A \le 0$ cannot be extended into the range $-1 \le A < -1/2$.

Then the localized discrete eigenfunctions for the eigenvalue problem (2), or equivalently, for any of Eqs. (12) and (13), corresponding to the discrete spectrum, may be defined for each interval of the constant potential (22), and then matched at the boundaries. As a result the discrete spectrum is determined by

$$\exp(2L\sqrt{\lambda^2 - A(1+A)}) = \frac{\dfrac{A}{2\lambda\sqrt{\lambda^2 - A(1+A)}} - \dfrac{\lambda}{\sqrt{\lambda^2 - A(1+A)}} + 1}{\dfrac{A}{2\lambda\sqrt{\lambda^2 - A(1+A)}} - \dfrac{\lambda}{\sqrt{\lambda^2 - A(1+A)}} - 1}, \tag{26a}$$

or alternatively by

$$\tan s = \frac{2s\sqrt{G - s^2}}{U - 2(G - s^2)}, \tag{26b}$$

where $s^2 = G(1-\mu^2)$, $\lambda L = \mu\sqrt{G}$, $U = AL^2$, $G = U(1+A)$, and $A(1+A) \neq 0$.

Some other forms of the solution (26) are given in the Appendix. In Eq. (26b) μ is the normalized eigenvalue, which is complex valued in the general case, and s is an auxiliary variable, which may also be complex valued.

The real parameter G is a convenient parameter, defining the strength of nonlinear effects, and generalizes the Ursell number U, defined here as $U = AL^2$, which is a commonly used similarity parameter for the KdV equation. Note that G tends to U when $|A|$ is small. In the opposite case, when $|A|$ is large, $G \to A^2L^2$. It is important to note that the RHS of Eq. (26) does not depend on L. This fact allows us to express value $G^{1/2}$ via the normalized eigenvalue μ and amplitude A of the disturbance,

$$\sqrt{G} = \frac{1}{\sqrt{1-\mu^2}}\left(\pi k + \operatorname{atan}\left[\mu\frac{\sqrt{1-\mu^2}}{\dfrac{U}{2G} - \mu^2}\right]\right),$$

$$\sqrt{G} = L\sqrt{A(1+A)}, \quad \mu = \frac{\lambda}{\sqrt{A(1+A)}}, \quad \frac{U}{2G} = \frac{1}{2(1+A)}. \tag{27}$$

In Eq. (27) the domain of the atan function lies within the interval $(-\pi/2, \pi/2)$; many branches of the solution exist due to the term πk, where k is an integer number.

In the sequel, two different cases corresponding to the sign of the disturbance are considered in detail.

A. Positive initial disturbance

When $A > 0$, then all the eigenvalues λ or μ are real and only solitary waves arise. This is an immediate consequence of Eq. (23), since if $\lambda_I \neq 0$ there is a contradiction when $A > 0$. Since here $G > 0$ it can be shown that the auxiliary variable s must also be real and positive, and so $0 < \mu < 1$. The solution of Eq. (26b) can now be analyzed qualitatively by plotting the curves of the left-hand side (LHS) and RHS as functions of real s. For this case of positive A it is more convenient to plot the inverse values of RHS and LHS of Eq. (26b). While the function $\cot s$ on LHS becomes infinite at $s = \pi k$, where k is integer, the inverse RHS of Eq. (26b) becomes infinite when $s = 0$ or $s = G^{1/2}$. Thus, at least one solution (one soliton) always exists for $A > 0$ for any $L > 0$. A new soliton branch appears when $G^{1/2} = \pi(N_s - 1)$, where N_s is the number of solitons given by

$$N_s = \left[\frac{\sqrt{G}}{\pi}\right] + 1, \tag{28}$$

where $[f]$ is the maximum integer not exceeding f.

When the KdV limit $A \to 0$ is concerned, the number of solitons N_s depends on the Ursell parameter only ($G \to U$). In the case of large amplitudes, N_s depends on parameter L^2A^2.

The solution (27) is plotted in Fig. 3. Each soliton branch starts with

$$\mu_0 = 0 \quad \text{at} \quad \sqrt{G_0} = \pi(N_s - 1) \tag{29}$$

and tends to $\mu_* = 1$ [otherwise, $\lambda \to \lambda_* = (A(1+A))^{1/2}$] when G tends to infinity. When the eigenvalue is small, the expression (27) may be decomposed into the Taylor series, and then the following relation holds, where a soliton level appears:

$$\mu \approx \frac{\sqrt{G} - \sqrt{G_0}}{2(1+A)}, \quad \text{when} \quad \mu \approx \mu_0. \tag{30}$$

The angle of the curve on the plane μ versus $G^{1/2}$ is defined by the value $(1+A)^{-1}$. It tends to zero when A is large, as shown in Fig. 3(c).

B. Negative initial disturbance

Let us first consider the case $A < -1$, when $G > 0$, but $U < 0$. At first we again examine Eq. (26b) for real values of s, when of necessity we must then have $s^2 < G$ corresponding to a real-valued eigenvalue. Then as in the previous case, the RHS and LHS of Eq. (26b) may be drawn as functions of s for a qualitative analysis, where here the curves are not inverted. The RHS curve has a "loop" which begins at $s = 0$ and

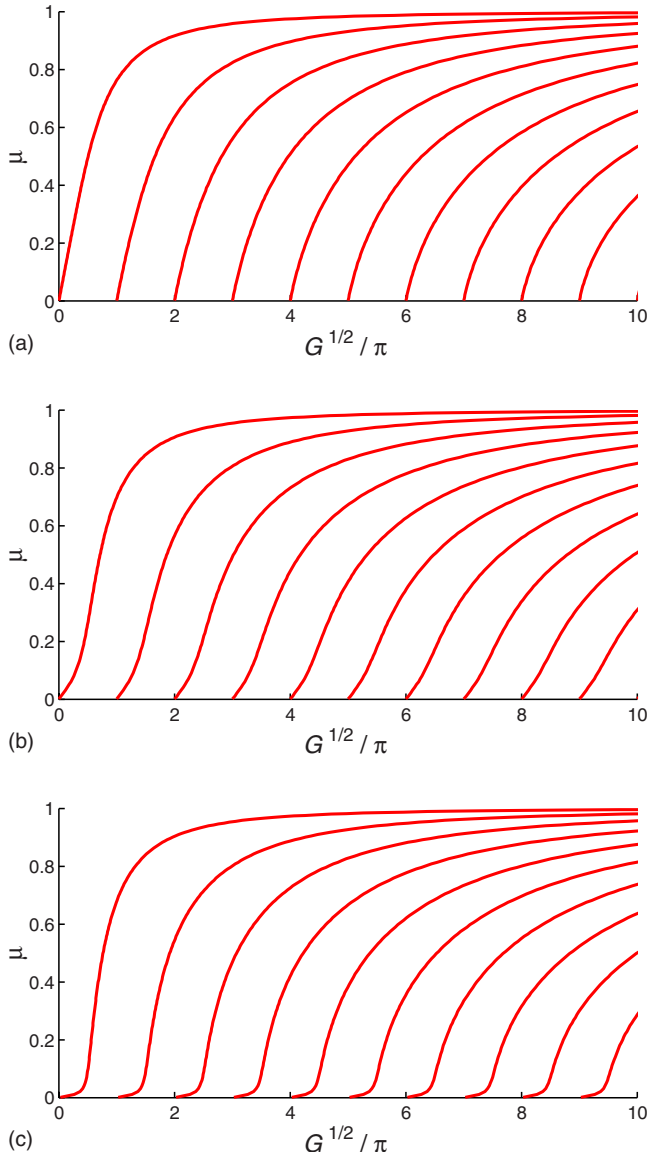

FIG. 3. (Color online) Normalized eigenvalues μ vs normalized nonlinear parameter $G^{1/2}/\pi$ for the cases (a) $A=0.5$, (b) $A=5$, and (c) $A=50$.

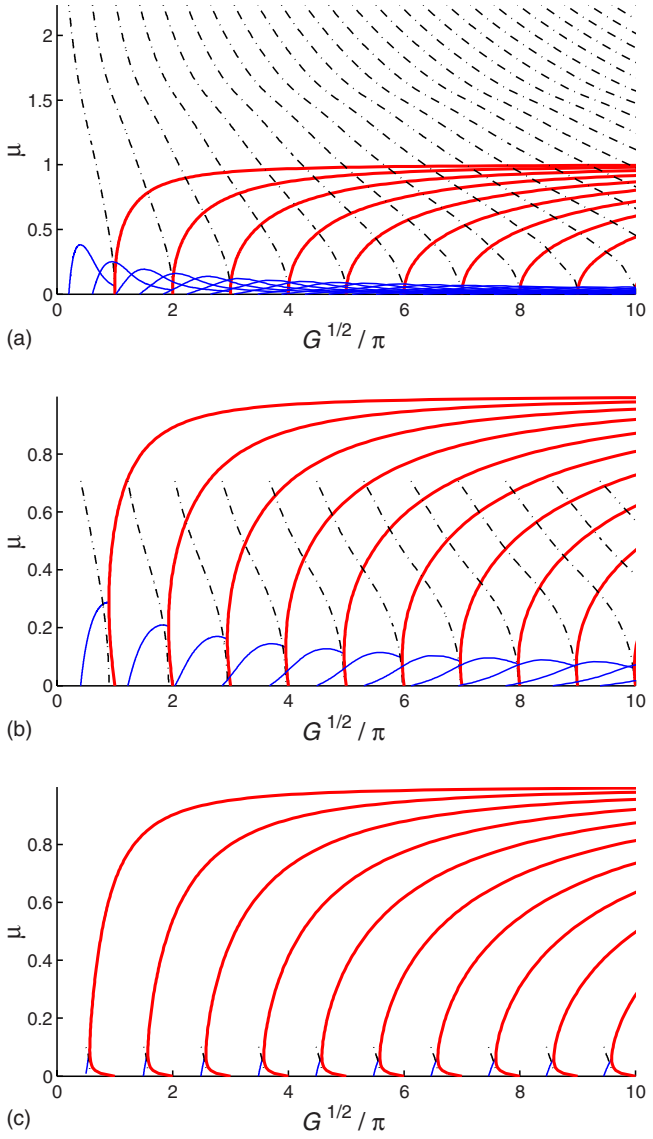

FIG. 4. (Color online) Normalized eigenvalues μ vs normalized nonlinear parameter $G^{1/2}/\pi$ for the cases (a) $A=-1.1$, (b) $A=-2$, and (c) $A=-50$. Red thick solid lines represent real eigenvalues; the complex eigenvalues are given by blue thin solid lines (the real part) and black thin dashed-dotted lines (the positive imaginary part).

ends at $s=G^{1/2}$. The RHS and LHS curves do not intersect if G is small. When G is close to, but less than the value

$$\sqrt{G_0}=\pi n, \quad n=1,2,\ldots, \tag{31}$$

two solutions of Eq. (26) exist with real eigenvalues, which is due to the two intersections of the curves. When G increases, one of the eigenvalues increases, while the other one decreases and vanishes at the threshold (31). The former eigenvalue continues growing and tends to $\mu_*=1$ [that is $\lambda \to \lambda^*=(A(1+A))^{1/2}$] when $G\to\infty$.

The situation is shown in Fig. 4, where we plot the normalized eigenvalue μ versus the normalized nonlinear parameter $G^{1/2}$ for three different values of negative amplitudes A (red thick solid curves). The points, when "soliton" branches start (with small eigenvalues), are defined by the condition (31), where n numerates the branches; at these points $\mu_0=0$. Two eigenvalues corresponding to two solitons can be readily seen in Fig. 4(c) (red thick solid curves), and less evident in Figs. 4(a) and 4(b).

When G becomes smaller, the two real eigenvalues merge and produce two complex conjugate eigenvalues. The blue thin solid curve and the black dashed-dotted curve in Fig. 4 show the real and positive imaginary parts of the numerical solution of Eq. (26). A pair of complex conjugate eigenvalues describes a breather (20). Close to the bifurcation point, the imaginary parts of the eigenvalues are small, but become larger when G decreases; at the same time the real part becomes smaller and vanishes at some point. If we suppose that the eigenvalue is pure imaginary, Eq. (26b) consists of real LHS and imaginary RHS, what can only be the case if they both are zero (when there is no solution) or infinite. The latter condition is

$$\mu_{\rm im}^2=\frac{U}{2G}=\frac{1}{2(1+A)}, \tag{32}$$

otherwise, $\lambda_{\rm im}^2=A/2$.

The expression (32) defines the upper limit of imaginary parts of μ, shown in Fig. 4. Since the LHS of Eq. (26b) is infinite, then $s=\pi/2+\pi k$, where k is an integer. Thus, with the use of Eq. (32), we get that

$$G_{\text{im}} = \frac{2(1+A)}{(1+2A)}\left(\frac{\pi}{2}+(n-1)\pi\right)^2, \tag{33}$$

where the integer $n>0$ numerates the branches. This nonlinear parameter corresponds to the case when the eigenvalues (λ and μ) are purely imaginary. It then follows from Eqs. (32) and (33) that complex solution exists when $A<-1$.

When $|A|$ is large, Eq. (33) becomes

$$G_{\text{im}}^{1/2} \approx \frac{\pi}{2}+(n-1)\pi, \quad -A \gg 1. \tag{34}$$

Thus, the real parts of the complex eigenvalues in Fig. 4(c) cross the abscissa axis at Eq. (34), which is in the middle between the points where the real eigenvalues are born ($G_0^{1/2}$). This limit corresponds to the case of the modified KdV equation. It is seen from Fig. 4 that the curves of real eigenvalues (thick lines) become close to the point defined by Eq. (34), when $|A|$ is large. It is well known that the relation (34) defines the birth of solitons within the framework of the mKdV equation. The large-amplitude limits for positive and negative values of A have similar solutions, compare Fig. 4(c) and Fig. 3(c).

For small values of $|1+A|$ the coefficient $(1+A)/(1+2A)$ in formula (33) becomes smaller, and hence the curves of complex eigenvalues become dense, see Figs. 4(a) and 4(b). This coefficient tends to zero when $A\to-1$. The bifurcation point, when two solitons tend to a breather, may be found approximately under certain assumptions (see the details in the Appendix) as

$$G_{\text{bif}}^{1/2} \approx n\pi - \frac{2}{n\pi}(1+A)^2, \quad \mu_{\text{bif}} \approx -2\frac{1+A}{\pi n}. \tag{35}$$

It may be seen in Fig. 4 that for small values of $|1+A|$ the real parts of the normalized complex eigenvalues corresponding to the bifurcation points become smaller as the branch number increases, but the bifurcation eigenvalue λ_{bif},

$$\lambda_{\text{bif}} \approx -2(1+A)\left(1-2\left(\frac{1+A}{\pi n}\right)^2\right), \tag{36}$$

slightly grows with the branch number n.

Let us now examine the case $-1\le A<-1/2$, when $G<0$, and $U<0$. We notice first that the reference solution corresponding to purely imaginary eigenvalues still exists, since formulas (32) and (33) remain valid and provide λ_{im} and G_{im}. In the present case $-1\le A<-1/2$ the values λ_{im} are imaginary, but s_{im} and μ_{im} are real. Moreover, it follows from Eq. (26) that purely imaginary eigenvalues λ_{im} exist even for the case $A=-1$. Indeed in this case, the expression (26a) collapses to

$$\exp(-2\lambda L) = 1+4\lambda^2. \tag{37}$$

It readily follows that Eq. (37) possesses purely imaginary solutions

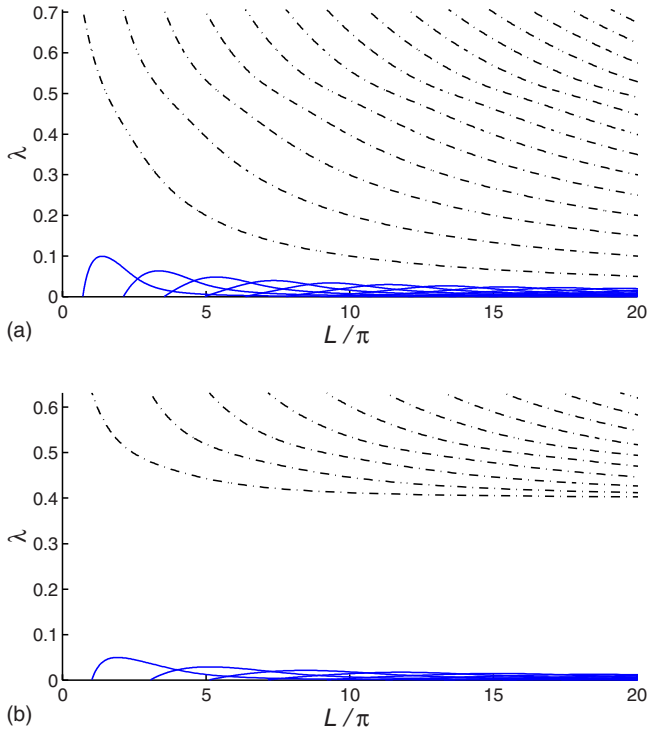

FIG. 5. (Color online) Eigenvalues λ vs normalized perturbation width L/π for the cases (a) $A=-1$ and (b) $A=-0.8$. The complex eigenvalues are given by blue thin solid lines (the real part) and black thin dashed-dotted lines (the positive imaginary part).

$$\lambda_{\text{im}} = \pm\frac{i}{\sqrt{2}}, \quad L_{\text{im}} = \frac{1}{\sqrt{2}}(\pi+2\pi n), \quad n>0, \quad (A=-1), \tag{38}$$

which agrees with Eqs. (32) and (33). A perturbation approach may now be used to prove the existence of the solution of Eq. (37) in the vicinity of λ_{im}. Let us seek a solution in the form

$$\lambda = \lambda_{\text{im}} + \lambda_R' + i\lambda_I', \quad L = L_{\text{im}} + l, \tag{39}$$

where λ_R', λ_I', and l are real and small; $\lambda_R'\ge 0$. Then a solution of Eq. (37) at the leading order is

$$\lambda_R' \approx \frac{2}{8+L_{\text{im}}^2}l, \quad \lambda_I' \approx -\frac{1}{\sqrt{2}}\frac{L_{\text{im}}}{8+L_{\text{im}}^2}l, \quad (A=-1). \tag{40}$$

Numerical solutions of Eq. (26) for the cases $A=-1$ and $A=-0.8$ are given in Fig. 5. Note that Fig. 5 is plotted in different coordinates than in Fig. 4. The maximum value of the imaginary part of the eigenvalues is given by Eq. (32), and they become smaller as the real part becomes nonzero, according to Eq. (40). Every branch of the complex eigenvalue tends to zero, when $L\to\infty$ and $A=-1$ [Fig. 5(a)], or to some purely imaginary value when $L\to\infty$ and $-1<A<-1/2$, as is readily seen in Fig. 5(b). This value is defined by the condition $\lambda^2-A(1+A)=0$, which is a solution of Eq. (26), as may be readily confirmed. Thus, the limiting value in Fig. 5(b) is defined by

$$\lambda^* = \pm i\sqrt{-A(1+A)}. \tag{41}$$

When $A=-1$, then $\lambda^*=0$, as seen in Fig. 5(a). When $A\to -1/2$, then λ^* tends to λ_{im}, and the solution vanishes.

IV. NUMERICAL SIMULATIONS

In this section the initial-value problem within the framework of the GE is solved by direct numerical integration of Eq. (1). The box-like disturbance (22) is used as the initial condition. From Sec. III, a disturbance of positive polarity will evolve in a qualitatively simple manner, producing sequences of solitary waves, which are similar to the solitons of the KdV equation, when their amplitudes are small, and similar to solitons of the modified KdV equation, when they are large. Negative disturbances, in contrast, can give birth to both solitons and breathers.

The regions near the bifurcation points on the plots in Fig. 4, where two real eigenvalues merge and produce a complex conjugate pair, are the most fascinating. In particular, the solution of the scattering problem for the eigenvalues alone does not give information about the polarity of the solitons. Here we consider only the case near the bifurcation point corresponding to the first branch of soliton solutions. We consider initial conditions for one amplitude, $A=-2$, but different widths, L [Fig. 4(b) corresponds to these conditions]. According to the solution presented in Sec. III, a breather appears when $G_{\text{im}}<G<G_{\text{bif}}$. The value of the width, corresponding to the bifurcation point, may be found from the estimate (35) for $A=-2$ as $L_{\text{bif}}\approx 1.8$, but in fact is underestimated. According to Fig. 4(b), it is about $G_{\text{bif}}\approx 0.90$ and $L_{\text{bif}}\approx 2.0$. Thus, a breather should appear when $0.9<L<2.0$. The IST predicts that two solitons should emerge within the interval $G_{\text{bif}}<G<G_0$, which in terms of the perturbation width results in $2.0<L<2.2$. Figure 6 shows the results of the direct numerical simulations of the GE (1) with initial conditions in form (22) for $A=-2$ and three values of the width, $L=1.9$ [Fig. 6(a)], $L=2$ [Fig. 6(b)], and $L=2.1$ [Fig. 6(c)].

The pseudospectral numerical code employs a three-layer integration in time. The computational domain is $-100<x<60$; an exponential damping is applied near the left boundary to suppress the fast dispersive tail radiation moving to the left. 4096 grid points are used. The time step is chosen small enough to provide a smooth evolution of the wave field. Velocities of the solitons and breathers, which should appear from the initial disturbances following the solution of the scattering problem, are given in Fig. 7. There the thick red line corresponds to the solitary wave branch, the thin blue line shows the "group" velocity of the breathers V. The vertical dashed lines from left to right correspond to the conditions of the numerical experiments, $L=1.9$, $L=2$, and $L=2.1$. Figure 6(a) shows the birth of a breather wave, which almost does not propagate in accordance with Fig. 7. An oscillating tail may be seen at the early stage of the evolution, but it quickly propagates to the left and is suppressed near the left boundary due to the introduced damping.

Two solitary-like waves propagating to the right may be seen in Fig. 6(b) at early times. One wave, of negative polarity appears first, and the second one of positive polarity and much smaller amplitude, appears later. The solitons collide at $t\approx 42$ when a transient intense positive wave occurs. Then the solitons restore their shapes, but the negative soli-

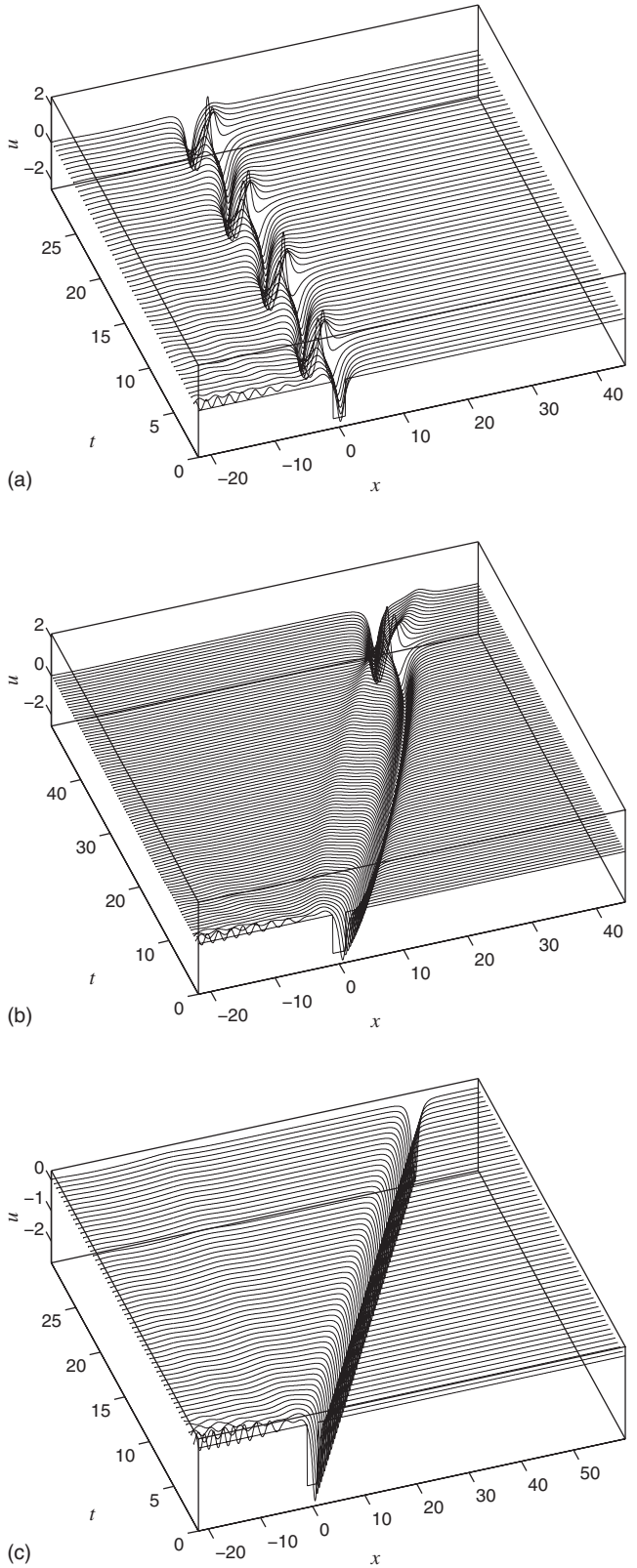

FIG. 6. Numerical simulation of the Cauchy problem for the GE and box-like initial perturbation of height $A=-2$ and widths (a) $L=1.9$, (b) $L=2$, and (c) $L=2.1$. Note the different scales of the figures.

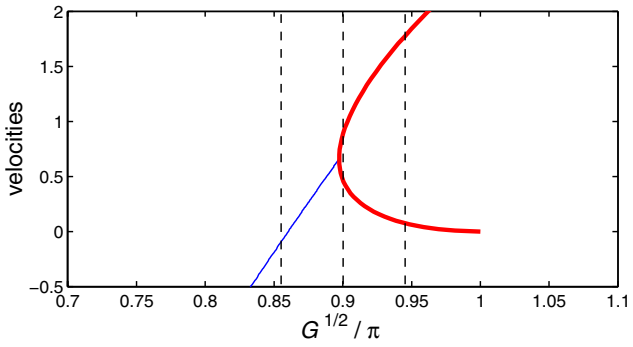

FIG. 7. (Color online) Velocities of solitons (thick red line) and breathers (thin blue line) for the case $A=-2$. Vertical dashed lines show conditions of the numerical experiments $L=1.9$, $L=2$, and $L=2.1$.

ton is shifted backward, while the positive one is shifted forward. This is a typical dynamics of a breather consisting of two coupled solitarylike waves (that is, a very small imaginary part of the eigenvalues), see Ref. 6. From Fig. 7, one could expect two solitary waves, while the direct numerical simulation shows coupled solitons composing a breather. This discrepancy may be because of small numerical errors due to the discretization (note that the case $A=-2$, $L=2$ is very close to the bifurcation point), or due to weak numerical viscosity leading to the coupling of solitons, similar to the experiments in Ref. 14.

In the case shown in Fig. 6(c), the solution of the AKNS problem predicts two solitary solutions (see Fig. 7, the vertical line on the right). The negative soliton is well seen, it corresponds to the larger value of the eigenvalue (and, correspondingly, to the larger velocity). The positive soliton is almost invisible in Fig. 6(c), it propagates very slowly, so that it is still near $x\approx 0$ after 30 time units of evolution.

V. CONCLUSION

We have investigated the initial-value problem for the GE with an initial disturbance of a simple box-like shape. The most interesting result of our study is the complicated evolution when the disturbance is negative. Near the bifurcation point, depending on weak variations in the initial disturbance, one soliton, two solitons, or a breather may be born, see Figs. 4–6. We should note, however, that when a pair of solitons belonging to one soliton branch of the AKNS problem results from a negative disturbance, the positive soliton is much smaller and is much slower propagating [see Figs. 6(b) and 6(c)]. Moreover, due to weak effects of nonintegrability in the numerical scheme, a pair of solitons may fuse and produce a breather.

The bifurcation point when the two solitons give birth to a breather corresponds to a rational breather was discussed in Ref. 9. Negative solitons with small eigenvalues are close to algebraic solitons, which are known to be structurally unstable.[9] It was shown in Ref. 9 that a perturbed negative soliton with a small eigenvalue may transform either into a negative soliton with a perturbed eigenvalue; or into a couple of solitons depending on the polarity of the perturbation; a negative soliton corresponding to the larger eigenvalue; and a positive soliton corresponding to the smaller eigenvalue; otherwise the perturbed solitary wave transforms to a breather solution. Thus, the destruction of an algebraic soliton leads to the formation of the same sets of waves, as we have found in the present study.

Note that depending on their parameters, breathers may propagate faster than linear waves, similar to solitons, or slower than solitons, and thus, may have the same speed as linear waves of an appropriate wavelength. But, in contrast to linear waves, breathers remain localized and preserve energy. Thus, in the ocean, internal breathers may significantly change the wave energy transport from zones of intense internal wave generation.

For the conditions of the stratified ocean when the contributions of the quadratic and cubic nonlinear terms to the internal wave dynamics are comparable (this depends on the specific density and current stratification), the initial-value problem for intense disturbances may be quite complicated. In contrast to the classic situation, when the field evolves according to the KdV theory, the evolution of a long-scale internal wave may result in the generation of solitary waves of both polarity, and breathers, which may be represented as coupled solitonlike waves of different signs, or as an intense wave group. Thus, the interpretation of observed internal waves can be a quite sophisticated problem.

ACKNOWLEDGMENTS

The study was supported by RFBR (Grant Nos. 08-05-91850, 09-05-90408, and 08-02-00039), and by NWO-RFBR Grant No. 047.017.2006.003.

APPENDIX: ANALYSIS OF COMPLEX EIGENVALUES

With the help of a trigonometric substitution

$$s=\sqrt{G}\sin\varphi, \tag{A1}$$

Eq. (26b) may be reduced to forms

$$A(\cot\varphi+\cot s)+(\cot 2\varphi+\cot s)=0 \tag{A2}$$

or

$$2A+1+\frac{\tan\varphi}{\tan(\varphi+s)}=0, \tag{A3}$$

and the normalized eigenvalue is defined by

$$\mu=\cos\varphi. \tag{A4}$$

Forms (A2) and (A3) are convenient to analyze the case $A<0$ when complex eigenvalues exist. It may be straightforwardly obtained that the origins of the solitary branches correspond to conditions

$$\varphi_0=\frac{\pi}{2}+\pi n, \tag{A5}$$

where integer $n>0$ numerates the branches. The maximum limit of the eigenvalues is attained when

$$\varphi\to\varphi_*=0. \tag{A6}$$

Complex eigenvalues require the phase φ to be complex.

If one supposes the eigenvalue to be complex with a small imaginary part, solution (A3) may be written in Taylor series in the form

$$T_1 + iT_2\,\mathrm{Im}(\varphi) + O(\mathrm{Im}(\varphi)^2), \tag{A7}$$

where T_1 and T_2 are real functions of $\mathrm{Re}(\varphi)$. Thus, condition $T_1=0$ defines the leading order of the solution (considerable real part of the eigenvalue) and is equivalent to Eq. (A3), and $T_2=0$ defines the condition, when this situation (small imaginary part of the eigenvalue) occurs, what reads

$$1 + \sqrt{G}\cos\varphi + \frac{1+2A}{1+4A(1+A)\cos^2\varphi} = 0, \tag{A8}$$

otherwise

$$Z^3 + Z^2 + \frac{G}{4A(1+A)}Z + \frac{G}{2A} = 0, \quad Z = \mu\sqrt{G}. \tag{A9}$$

Equation (A9) defines the bifurcation points jointly with Eq. (26). The solution of Eq. (A9) may be found, but Eq. (26) remains transcendental.

It may be shown through differentiation that Eq. (A3) results in Eq. (A8) when condition

$$\frac{\partial G}{\partial \varphi} = 0 \tag{A10}$$

is employed. It follows from the graphical solution of Eq. (26b) that near the bifurcation points $s \approx \pi n$, $Nr \approx \pi^2 n^2$, and thus, $\varphi \approx \pi/2$. Then, the RHS of solution (27) may be decomposed in the Taylor series for $\varphi \approx \pi/2$ as

$$\sqrt{G} = \pi n - 2(1+A)\left(\varphi - \frac{\pi}{2}\right) + \frac{\pi n}{2}\left(\varphi - \frac{\pi}{2}\right)^2 + O\left(\left(\varphi - \frac{\pi}{2}\right)^3\right). \tag{A11}$$

The first three terms on the RHS of Eq. (A11) represent a parabola with the minimum corresponding to the condition (A10), which therefore corresponds to the bifurcation point,

$$\varphi_{\mathrm{bif}} \approx \frac{\pi}{2} + 2\frac{1+A}{\pi n}, \tag{A12}$$

which gives formula (35).

[1] L. A. Ostrovsky and Yu. A. Stepanyants, Chaos **15**, 037111 (2005).
[2] K. R. Helfrich and W. K. Melville, Annu. Rev. Fluid Mech. **38**, 395 (2006).
[3] *Solitary Waves in Fluids*, edited by R. H. J. Grimshaw (WIT, Southampton, 2007).
[4] P. G. Drazin and R. S. Johnson, *Solitons: An Introduction* (Cambridge University Press, Cambridge, England, 1996).
[5] A. V. Slyunyaev and E. N. Pelinovskii, Sov. Phys. JETP **89**, 173 (1999).
[6] A. V. Slyunyaev, Sov. Phys. JETP **92**, 529 (2001).
[7] R. Grimshaw, D. Pelinovsky, E. Pelinovsky, and A. Slunyaev, Chaos **12**, 1070 (2002).
[8] R. Grimshaw, E. Pelinovsky, and T. Talipova, Nonlinear Processes Geophys. **4**, 237 (1997).
[9] D. Pelinovsky and R. Grimshaw, Phys. Lett. A **229**, 165 (1997).
[10] K. W. Chow, R. H. J. Grimshaw, and E. Ding, Wave Motion **43**, 158 (2005).
[11] R. Grimshaw, E. Pelinovsky, T. Talipova, M. Ruderman, and R. Erdélyi, Stud. Appl. Math. **114**, 189 (2005).
[12] K. G. Lamb, O. Polukhina, T. Talipova, E. Pelinovsky, W. Xiao, and A. Kurkin, Phys. Rev. E **75**, 046306 (2007).
[13] S. V. Dmitriev and T. Shigenari, Chaos **12**, 324 (2002).
[14] D. N. Ivanychev and G. M. Fraiman, Theor. Math. Phys. **110**, 199 (1997) [in Russian, Teoreticheskaya i Matematicheskaya Fizika **110**, 254 (1997)].
[15] R. Grimshaw, D. Pelinovsky, E. Pelinovsky, and T. Talipova, Physica D **159**, 35 (2001).
[16] R. Grimshaw, E. Pelinovsky, and T. Talipova, Physica D **132**, 40 (1999).
[17] S. V. Manakov, Zh. Eksp. Teor. Fiz. **65**, 505 (1973) [Sov. Phys. JETP **38**, 248 (1974)].
[18] J. Satsuma and N. Yajima, Suppl. Prog. Theor. Phys. **55**, 284 (1974).
[19] Z. V. Lewis, Phys. Lett. A **112**, 99 (1985).
[20] J. Burzlaff, J. Phys. A **21**, 561 (1988).
[21] H. Takahashi and K. Konno, J. Phys. Soc. Jpn. **58**, 3085 (1989).
[22] D. J. Kaup, J. El-Reedy, and B. A. Malomed, Phys. Rev. E **50**, 1635 (1994).
[23] D. J. Kaup and B. A. Malomed, Physica D **84**, 319 (1995).
[24] M. Desaix, D. Anderson, M. Lisak, and M. L. Quiroga-Teixeiro, Phys. Lett. A **212**, 332 (1996).
[25] S. Clarke, R. Grimshaw, P. Miller, E. Pelinovsky, and T. Talipova, Chaos **10**, 383 (2000).
[26] M. Klaus and J. K. Shaw, Phys. Rev. E **65**, 036607 (2002).
[27] M. Desaix, D. Anderson, L. Helczynski, and M. Lisak, Phys. Rev. Lett. **90**, 013901 (2003).
[28] M. J. Ablowitz, D. J. Kaup, A. C. Newell, and H. Segur, Stud. Appl. Math. **53**, 249 (1974).
[29] J. W. Miles, Tellus **31**, 456 (1979).
[30] M. Wadati, J. Phys. Soc. Jpn. **34**, 1289 (1973).
[31] N. N. Romanova, Theor. Math. Phys. **39**, 415 (1979) [in Russian, Teoreticheskaya i Matematicheskaya Fizika **39**, 205 (1979)].
[32] Y. Chen and P. L.-F. Liu, Wave Motion **24**, 169 (1996).
[33] J. Small, T. C. Sawyer, and J. Scott, Ann. Geophys. **17**, 547 (1999).